Available online at www.sciencedirect.com
ScienceDirect
Journal of Non-Crystalline Solids 353 (2007) 1741–1747
JOURNAL OF NON-CRYSTALLINE SOLIDS
www.elsevier.com/locate/jnoncrysol

Structural studies of lead aluminate glasses

E.R. Barney [a], A.C. Hannon [b,*], D. Holland [a], D. Winslow [c], B. Rijal [c], M. Affatigato [c], S.A. Feller [c]

[a] Department of Physics, University of Warwick, Coventry CV4 7AL, UK
[b] ISIS Facility, Rutherford Appleton Laboratory, Chilton, Didcot, Oxon OX11 0QX, UK
[c] Physics Department, Coe College, 1220 1st Avenue NE, Cedar Rapids IA 52402, USA

Available online 2 April 2007

Abstract

Lead aluminate melts were quenched rapidly with a roller quencher and bulk glasses were formed over a composition range from 72.5 to 80.0 mol% PbO. Pulsed neutron diffraction, ^{27}Al MAS NMR and Raman spectroscopy were used to study the structure of a series of these glasses. The results show that in the glasses the aluminium is four coordinated by oxygen across the compositional range, with a bond length of about 1.76 Å. The Pb–O peak in the neutron correlation function is asymmetric, and it can be modelled in terms of two bond lengths of ~2.25 Å and ~2.47 Å, with the majority of the coordination at the shorter distance. There is evidence that most or all of the lead ions are on asymmetric sites, coordinated by three oxygens in a trigonal pyramid arrangement. Both the neutron diffraction and Raman results indicate that the Pb–O bond lengths become shorter with increasing lead content.

PACS: 61.12.Ld; 61.18.Fs; 61.43.Fs; 78.30.Ly

Keywords: Neutron diffraction/scattering; Raman scattering; Heavy metal oxides; Oxide glasses; NMR, MAS NMR and NQR; Short-range order

1. Introduction

The lead aluminate glass system, $PbO–Al_2O_3$, has been little studied. It was first reported that the system was glass forming, over a significant range in composition, by Kantor et al. [1] who used the 'gun technique' for fast cooling of the melts [2]. It was noted that the formation of these glasses was assisted by the presence of a eutectic point at ~85 mol% PbO [3], which lowers the melting temperatures required and therefore reduces the problem of lead volatilization. Further work was carried out by Morikawa et al. [4] who used differential thermal analysis (DTA), X-ray diffraction (XRD) and infra-red (IR) spectroscopy to confirm glass formation, and dark field microscopy to identify the presence of minute crystallites. Kantor et al. [1] report the glass forming range to be 50–95 mol% PbO, whilst Morikawa et al. [4] found the same upper limit, but a different lower limit of 67 mol% PbO. The high PbO contents which have been reported indicate that lead is not acting purely as a modifier in these glasses.

The lead aluminate glass system is being studied as part of a broader investigation into lone pair ions in glass. The structural role of lone pair cations in glass is of interest due to the highly asymmetric coordinations which they often exhibit. The asymmetry of the lone pair ion environment results in the charge associated with the lone pair being highly polarizable, producing strong non-linear optical effects. By understanding the structure of the glass and the effect of composition on the extension of the lone pair cations, these optical properties can be better exploited.

There have been no previous structural studies of lead aluminate glasses, but studies of calcium aluminate glasses using XRD [5], nuclear magnetic resonance (NMR) [6], neutron diffraction [7] and molecular dynamics modelling [8] indicate that the aluminium, at these concentrations, should be four coordinated, while neutron diffraction work

* Corresponding author. Tel.: +44 1235 445358; fax: +44 235 445720.
E-mail address: a.c.hannon@rl.ac.uk (A.C. Hannon).

0022-3093/$ - see front matter © 2007 Elsevier B.V. All rights reserved.
doi:10.1016/j.jnoncrysol.2007.02.007

[9,10] and extended X-ray absorption fine structure (EXAFS) studies [11] on lead gallates, as well as NMR [12], XRD [13] and Raman spectroscopy [14] studies on lead silicates, suggest that the lead will be in either PbO_3 trigonal pyramids or PbO_4 square pyramids.

2. Neutron diffraction theory

A neutron diffraction experiment measures the differential cross section, $\frac{d\sigma}{d\Omega}$, which is equivalent to the total scattering from the sample, $I(Q)$, where $\hbar Q$ is the magnitude of the momentum transfer [15]. The total scattering is a sum of the self scattering (the interference between waves scattered from the same nucleus), $I^s(Q)$ and the distinct scattering, $i(Q)$ (the interference between waves scattered from different nuclei).

$$\frac{d\sigma}{d\Omega} = I(Q) = I^s(Q) + i(Q). \quad (1)$$

The self scattering can be calculated to a good approximation, and subtracted from the data to give the distinct scattering in reciprocal space, and the latter can then be Fourier transformed to give the total correlation function in real-space, given by

$$T(r) = T^0(r) + \frac{2}{\pi}\int_0^{Q\max} Qi(Q)M(Q)\sin(rQ)dQ, \quad (2)$$

where $T^0(r)$ is the average density contribution to the correlation function, and $M(Q)$ is a modification function introduced to reduce termination ripples in the Fourier transform, which arise as a consequence of the finite maximum experimentally accessible momentum transfer, Q_{max}.

The result of a diffraction experiment is not element-specific, and the total correlation function is a weighted sum of all possible partial correlation functions, $t'_{ll'}(r)$, broadened by convolution with the real-space resolution function, $P(r)$ [16].

$$T(r) = \sum_{l,l'} c_l \bar{b}_l \bar{b}_{l'} t'_{ll'}(r) \quad (3)$$

where c_l is the atomic fraction of element l, $\bar{b}_l$ is the coherent neutron scattering length for element l, and the double summation is over all the pairwise combinations of elements in the sample.

3. Experimental detail

3.1. Sample preparation

Samples were prepared at Coe College with nominal compositions of 72.5, 75.0, 76.7, 77.7, 80.0 and 82.5 mol% PbO. The chemicals used to produce the samples were Pb_3O_4 and Al_2O_3, of at least 99.9% purity. The compositional range of glasses made was limited by the rapidly increasing melting temperatures required as the compositions move away from the eutectic point [3]. The samples were melted in Pt–Rh crucibles at temperatures between 1000–1350 °C for 20 min. Weight loss measurements were then carried out to test for volatilization of the lead, before heating the samples for another 20 min and then pouring. The rapid cooling for the samples ($>10^5$ K s^{-1}) was achieved using a motorized roller quencher [17]. Weight loss measurements showed that up to 1 g was lost on heating an 18 g batch for 20 min. This is greater than the mass loss expected from the excess oxygen in the starting mixture (~0.4 g) and suggests that some lead volatilization has occurred. XRD was carried out to determine whether the samples were amorphous.

3.2. ^{27}Al MAS NMR

^{27}Al MAS (magic angle spinning) NMR was conducted using a Varian 600 spectrometer tuned to 156.36 MHz with spinning speeds of 12 kHz on a 3.2 mm Varian Chemagnetic probe. A single pulse program was used with a 2 s pulse delay and 0.5 μs pulse width. All the chemical shifts are referenced using yttrium aluminium garnet (0.7 ppm with respect to $Al(H_2O)_6^{3+}$).

3.3. Raman spectroscopy

Polarized (H–H) Raman spectra were recorded on a Jasco NRS-3100 microRaman spectrophotometer using a 785 nm SLM diode laser. The spectra from small glass fragments were collected over a frequency range of 25–1800 cm^{-1}, centering around 990 cm^{-1}.

3.4. Neutron diffraction

Neutron diffraction data were collected using the GEM diffractometer [18] at the ISIS pulsed neutron source, Rutherford Appleton Laboratory. Small fragments of the samples were used for the time of flight neutron diffraction measurements. These were held in 8.3 mm diameter vanadium cans with walls of thickness 25 μm.

4. Results

4.1. ^{27}Al MAS NMR

Fig. 1 shows the ^{27}Al MAS NMR data for the six lead aluminate samples. All the spectra have a peak at ~67 ppm, indicating the presence of aluminium which is four coordinated by oxygen. The two highest PbO content samples have a smaller second peak at ~14 ppm, corresponding to aluminium ions which are six coordinated by oxygen [19].

^{27}Al MAS NMR was also used for quantitative analysis of the sample compositions, by comparing the integrated intensities of the ^{27}Al MAS NMR spectra with that of α-Al_2O_3. The sample compositions were found to be in good agreement with the nominal compositions (see Table 1).

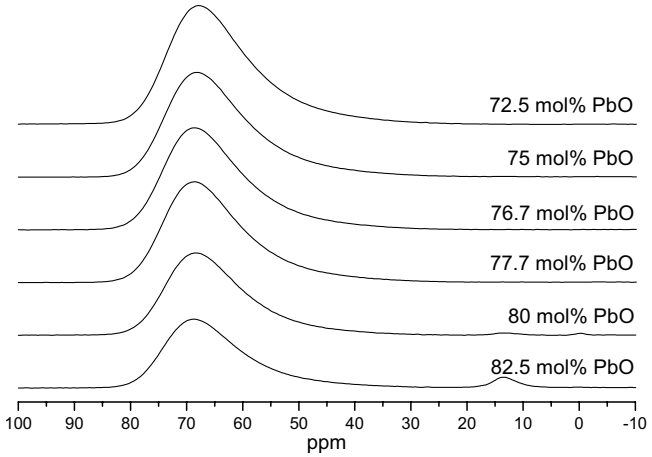

Fig. 1. The ^{27}Al NMR spectra for the six lead aluminate samples.

Table 1
The compositional analysis for the lead aluminate samples using ^{27}Al NMR

Nominal composition (mol% PbO)	Composition from ^{27}Al MAS NMR (mol% PbO) ±0.8
72.5	72.4
75	76.6
76.7	77.7
77.7	77.0
80	79.6
82.5	78.9

4.2. Raman spectroscopy

Three typical Raman spectra are shown in Fig. 2. The H–H Raman spectra are dominated by the lead related bond vibrations which occur below 200 cm^{-1} [14]. In this region there are two peak manifolds at 125 cm^{-1} and 50 cm^{-1}. The areas under the two features were integrated and the positions of the maxima found. Fig. 3(a) indicates

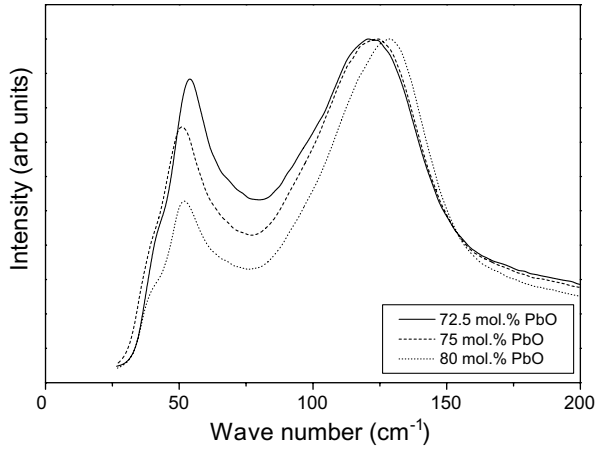

Fig. 2. Three H–H Raman spectra, normalized to the ~125 cm^{-1} manifold to demonstrate the shift in peak position with composition.

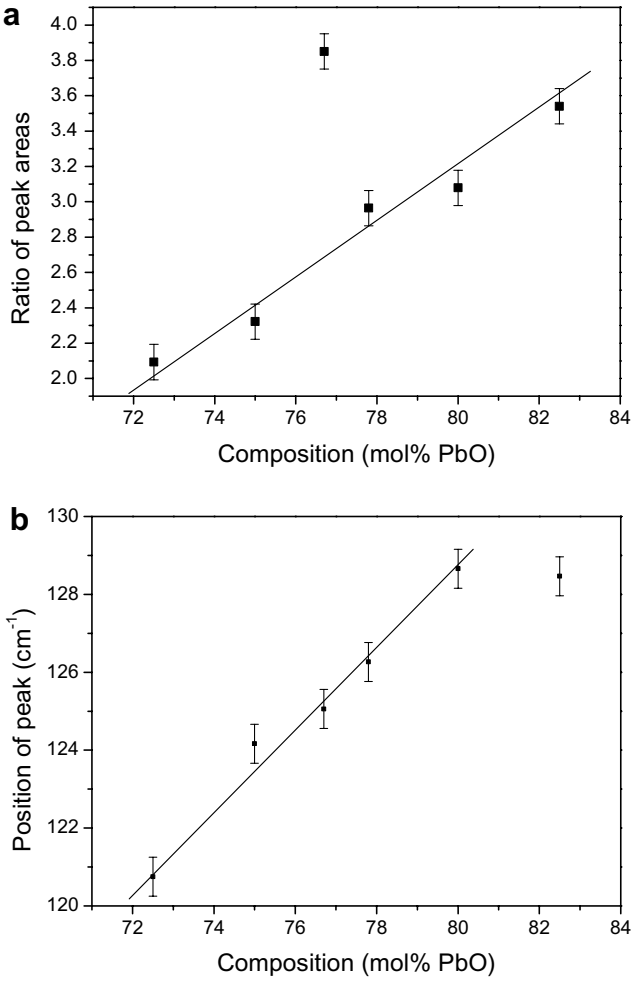

Fig. 3. (a) The ratio of the areas of the two low frequency manifolds in the H–H polarized Raman spectra, and (b) the position of the ~125 cm^{-1} manifold with composition.

that the area of the 125 cm^{-1} manifold, compared to the 50 cm^{-1} manifold, increases linearly across the compositional range. Fig. 3(b) shows the shift in the position of the manifold around ~125 cm^{-1} to higher frequencies, with increasing PbO content.

4.3. Neutron diffraction

An initial check of the neutron diffraction data for the six lead aluminate samples showed that the four with the lowest PbO content were completely amorphous. There was, however, slight crystallization of the 80 mol% PbO sample, and more substantial Bragg peaks in the data for the 82.5 mol% PbO sample; for this reason the neutron diffraction data for the latter were not processed further. This crystallization was not apparent in the XRD patterns.

The distinct scattering curves, $i(Q)$, after being fully corrected using a combination of the gudrun program [20] and the ATLAS suite of programs [16], are shown in Fig. 4(a) for the five samples without Bragg peaks. Oscillations were clearly visible out to a maximum momentum transfer,

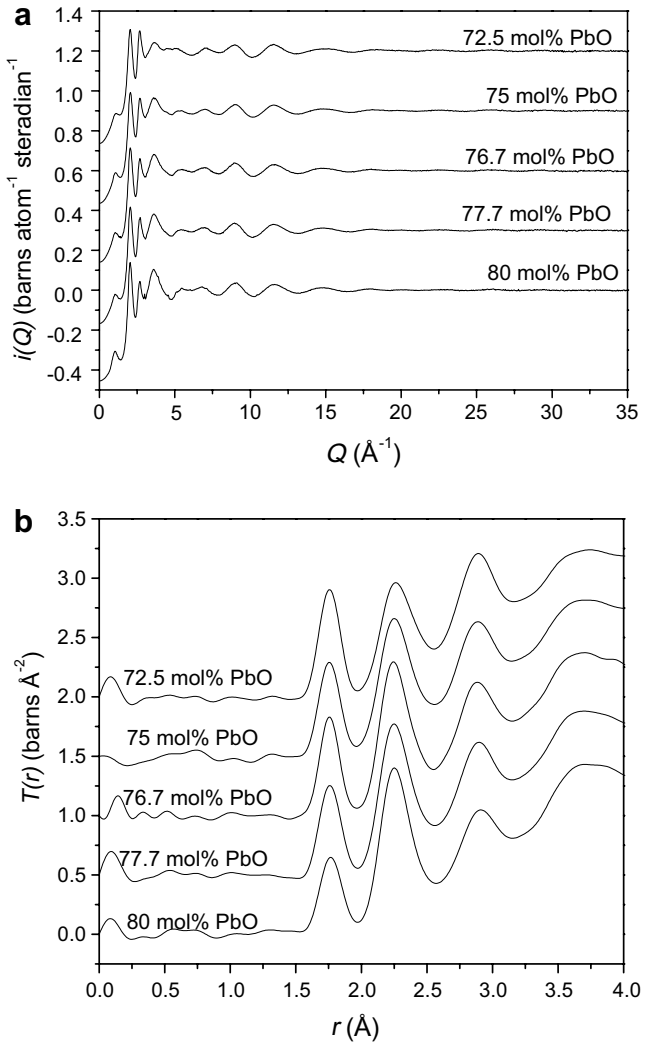

Fig. 4. The neutron diffraction data for the five lead aluminate glasses: (a) the distinct scattering, $i(Q)$ and (b) the total correlation function, $T(r)$.

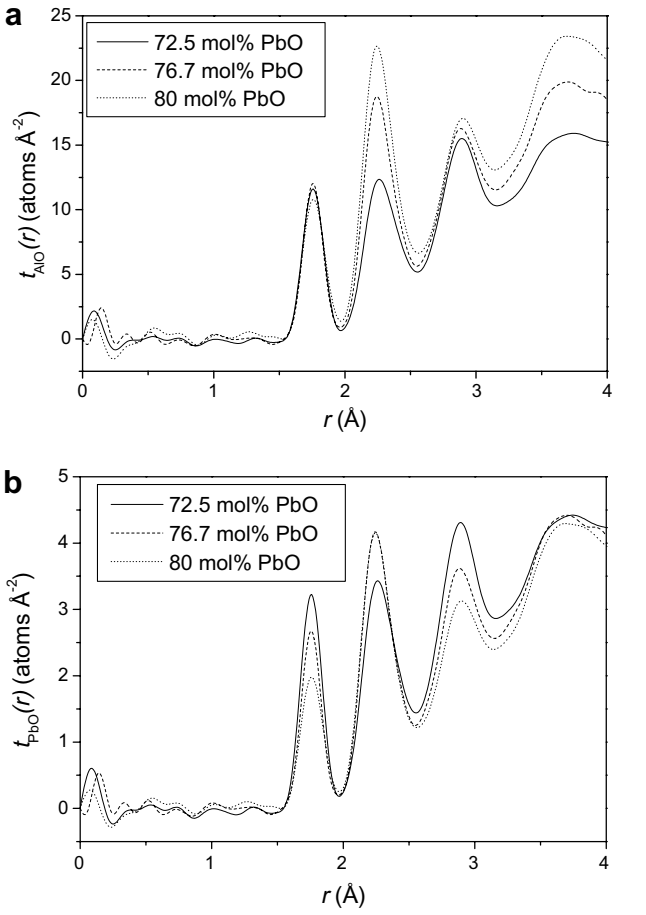

Fig. 5. The total correlation functions after scaling to give: (a) the Al–O partial correlation function, and (b) the Pb–O partial correlation function.

Q_{max}, of 35 Å^{-1} and a quadratic, of the form $A + BQ^2$, was fitted to the data at low Q to extrapolate $i(Q)$ down to $Q = 0$. A Fourier transform was carried out using the Lorch modification function [21] with a Q_{max} of 35 Å^{-1}. Fig. 4(b) shows the correlation functions, $T(r)$, which were obtained.

In the region of the X–O first peak (where X=Pb, Al) all other contributions, other than $t_{XO}(r)$ are equal to zero. Therefore, dividing $T(r)$ by the appropriate weighting factor $2c_x\bar{b}_x\bar{b}_o$ (see Eq. (3)) gives the partial X–O correlation function over the limited distance range of the relevant peak. Fig. 5 shows the result of dividing the total correlation function by the weighting factors for the Al–O and the Pb–O partial correlation functions. These plots reveal any changes in the bonding.

The correlation functions, $T(r)$, were fitted using Gaussian peaks convoluted with the real-space resolution function, $P(r)$, to obtain a series of peaks which allow the bond length, coordination number and disorder parameters for each short correlation to be extracted [22]. The peak fitting to $T(r)$ was carried out in two parts, with typical results for two of the samples shown in Fig. 6. Initially the first two peaks were fitted over a distance range to model the Al–O distance and the shorter Pb–O distances. A second smaller Pb–O peak is seen in the residual for this initial fit and this peak was fitted, along with the O–O peak, to give a further contribution to the Pb–O coordination number, bringing it to approximately 3. Table 2 details the coordination numbers, bond lengths and disorder parameters extracted for the first Al–O, Pb–O and O–O peaks.

5. Discussion

The range in composition over which we were able to form lead aluminate glasses was from 72.5 mol% to 80.0 mol% PbO. Although previous workers [1,4] have reported a high lead limit to the glass forming range of 95 mol% PbO, we could not make a good bulk glass beyond 80.0 mol% PbO without crystallization. Kantor et al. [1] do not give details of the method for glass melting, but Morikawa et al. [4] state that the glasses were held at melt temperature for only a few seconds, reducing the problem of volatilization. To achieve this, the samples were

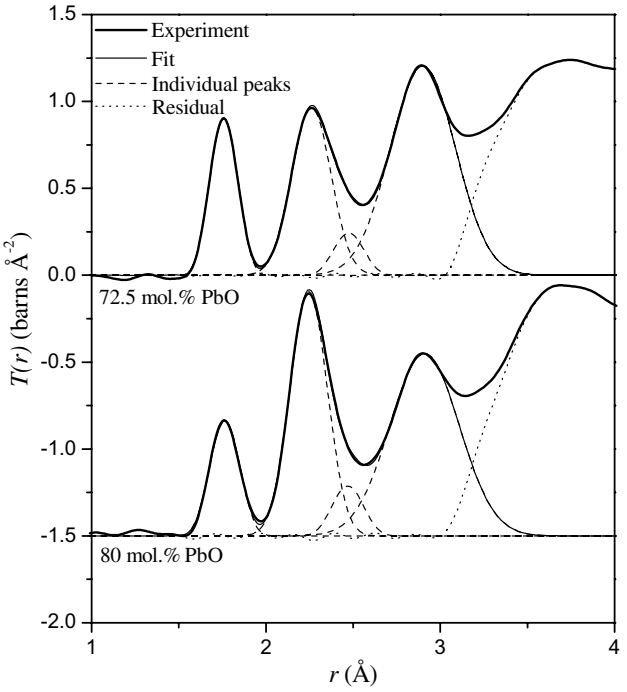

Fig. 6. Fits to the total correlation function, $T(r)$, for the lowest and highest PbO content (the curves for 80 mol% PbO are displaced by −1.5 units for clarity).

melted in a small platinum crucible of volume 20 mm^3. In making a larger quantity of glass, held at temperature long enough to ensure good mixing, we found the bulk glass forming limit to be 80 mol% PbO.

Hannon et al. [10] have calculated the number of bridging oxygens per gallium, n_{BO}, for the analogous lead gallate system, on the assumption that all oxygens are bonded to either one or two gallium atoms, and it was found that n_{BO} becomes zero for a composition of 83.3 mol% PbO. If lead aluminate glass can be made with more than 83.3 mol% PbO then there must be oxygens which are bonded only to lead atoms. A structure with such oxygens would be inconsistent with Zachariasen's rules for oxide glass formation [23], whereas the high PbO limit of glass formation which we have found is readily understood as occurring as the composition approaches a value for which all of the oxygens are bonded to only one aluminium. The glass forming limit which we found, 80 mol% Al_2O_3, corresponds to a value of one for n_{BO}, the number of bridging oxygens per aluminium.

From a structural point of view, it is expected that the lower limit of glass formation should be at the equimolar composition, at which point it is possible to form a fully connected tetrahedral Al–O network with no non-bridging oxygens. However, we found a lower glass forming limit of 72.5 mol% PbO. The glass formation was limited by the rapidly increasing melting point, as the composition moves away from the eutectic point, and the corresponding increase in lead volatilization.

^{27}Al MAS NMR and neutron diffraction both show evidence of crystal formation above 80.0 mol% PbO. The second, smaller peak in the NMR data for the 80.0 and 82.5 mol% PbO glasses shows that a second phase which contains six coordinated aluminium is present, and the position of the peak is very close to that for α-Al_2O_3, whose isotropic chemical shift parameter is ~16 ppm [19]. Furthermore, the neutron diffraction data show Bragg peaks which can be assigned to α-Al_2O_3. At 82.5 mol% PbO, above the upper limit for the formation of bulk glass, Bragg peaks corresponding to PbO (both massicot and litharge forms) were also present. This agrees with the dark field microscopy work of Morikawa et al. [4] which showed that, although mostly glassy, small crystallites were present in the high lead content glasses.

The neutron correlation functions (Fig. 4(b)) contain three peaks at low r and, by comparison with literature values, these peaks can be assigned to three different atomic correlations. The first peak is at a distance of 1.76 Å, a typical Al–O bond length. This is corroborated by the decrease in the area under the peak when the Al_2O_3 content of the composition is reduced. The second peak increases in size with increasing lead content and, with a peak position of 2.25 Å, can be assigned to the Pb–O correlation. The final peak is at a distance of 2.9 Å, and is due mainly to the O–O correlations. The change in peak intensities with composition gives further confirmation that the lead content in the nominal compositions is retained in the roller quenched glass samples, agreeing with the compositional analysis from quantitative ^{27}Al MAS NMR.

The neutron diffraction data (Table 2) show that, within an error of 0.1, the aluminium ions in the glass are four coordinated, independent of sample composition, and the Al–O distance is consistent with bond valence predictions [7] for four-coordination. The interatomic distance for the first O–O peak, for a tetrahedral AlO_4 network, should be $\sqrt{8/3}r_{Al-O} = 2.87$ Å. The bond length measured from

Table 2
The peak positions, thermal parameters and coordination numbers extracted for the Al–O, Pb–O and O–O peaks by fitting the total correlation function

Mol% PbO	Al–O			Pb–O (1)			Pb–O (2)			Pb–O	O–O
	r_{Al-O} (Å)	$\langle u^2_{Al-O}\rangle^{1/2}$ (Å)	n_{Al-O}	r_{Pb-O} (Å)	$\langle u^2_{Pb-O}\rangle^{1/2}$ (Å)	n_{Pb-O}	r_{Pb-O} (Å)	$\langle r^2_{Pb-O}\rangle^{1/2}$ (Å)	n_{Pb-O}	Σn_{Pb-O}	r_{O-O} (Å)
72.50	1.7632(5)	0.0554(7)	4.0(1)	2.260(3)	0.098(1)	2.180(4)	2.475(1)	0.063(3)	0.4532(3)	2.633(3)	2.900(1)
75.00	1.7638(7)	0.058(1)	3.8(1)	2.251(2)	0.101(2)	2.524(4)	2.490(2)	0.0687(2)	0.47(1)	2.99(1)	2.892(2)
76.50	1.7581(5)	0.0577(3)	4.0(1)	2.2463(4)	0.0925(1)	2.471(2)	2.468(3)	0.0655(3)	0.46(2)	2.93(2)	2.897(3)
77.50	1.7622(5)	0.05490(4)	4.0(1)	2.247(1)	0.090(1)	2.389(3)	2.471(2)	0.070(2)	0.52(1)	2.91(1)	2.908(2)
80.00	1.7639(7)	0.0625(1)	4.0(1)	2.245(1)	0.091(1)	2.498(2)	2.469(2)	0.068(2)	0.46(1)	2.96(1)	2.910(2)

$T(r)$ is 2.9 Å, slightly longer than anticipated, and this suggests that there is some other contribution to $T(r)$ at this distance. The normalized $t_{Al-O}(r)$ plot (Fig. 5(a)) indicates that the Al–O bonding does not significantly alter with composition.

When the Pb–O peak identified in $T(r)$ at 2.25 Å was fitted (Fig. 6), it was found to have a coordination number significantly less than three, the minimum value expected. When a shoulder in the residual from the initial fit was treated as a second smaller Pb–O peak, the coordination number increased to ~3. This indicates that there is a marked asymmetry to the Pb–O bond length distribution in the glass. The majority of bonds are short, having a length of ~2.25 Å, while a smaller fraction are longer. This is similar to the asymmetric Pb–O bonding observed in lead gallate glasses [9,10].

The $t_{Pb-O}(r)$ plot, shown in Fig. 5(b), indicates some variation in the Pb–O coordination with composition. For 72.5 mol% PbO the Pb–O peak has a smaller area than for the four other compositions, suggesting a lower coordination number for the lead and this is confirmed by the fit results for the two Pb–O peaks (Table 2). In addition to this, the Pb–O peak shifts to a slightly shorter bond length with increasing PbO content. The area of the 125 cm^{-1} peak in the Raman H–H spectra (Fig. 3(a)) increases strongly with composition. (The outlying point, for the 76.7 mol% PbO glass was measured for a very small fragment, and this may not have been representative of the bulk composition. Hence this point can be neglected.) Studies on lead silicate glasses [14] show that there is an H–H polarized peak at 138 cm^{-1} which behaves in a similar manner with increasing lead oxide content. This ~125 cm^{-1} peak can be assigned to the vibrations of the Pb–O bonds [14] and Fig. 3(b) shows a clear shift in frequency for this peak. The increase in frequency of the vibrations with increasing PbO suggests that the Pb–O bond lengths are becoming shorter and stronger [14], consistent with the neutron data.

There are found to be two very different types of coordination environment for the lone pair ion Pb^{2+} in divalent lead compounds [24]. The lead ion may be surrounded either by a symmetric distribution of ligands, or an asymmetric distribution of ligands with an identifiable void in the distribution of bonds to the ligands. For low coordination numbers (2–5) the environment is asymmetric with short bond lengths, whilst for high coordination numbers (9 and 10) the environment is symmetric with long bond lengths. For intermediate coordination numbers (6–8) both types of environment are found. The $PbO–Al_2O_3$ phase diagram [3] shows only one crystal phase at a composition close to the eutectic, and this is $Pb_9Al_8O_{21}$ [25] (with a composition ~69.3 mol% PbO). Al–O is tetrahedrally coordinated in this structure, with bond lengths similar to those observed in the glasses. The lead ions in crystalline $Pb_9Al_8O_{21}$ are located on three crystallographically unique sites, and both symmetric and asymmetric types of coordination are present. 11% of the Pb ions are on a site with a symmetric environment, a high coordination number ($n_{PbO} = 8$) and long Pb–O bond lengths (2.43 and 2.74 Å). The other two Pb sites have asymmetric environments based on a PbO_3 trigonal pyramid, with Pb–O bond lengths varying from 2.25 to 2.40 Å. The majority of the lead ions on asymmetric sites also have a longer Pb–O bond at 2.75 Å – similar in length to the bonds around the symmetric Pb site.

The fit results in Table 2 show that there are short Pb–O bonds in the glasses of length ~2.25 Å, and this is clear evidence that the glass contains asymmetric lead sites, because symmetric lead sites do not have such short bond lengths. The most common three coordinated lead site in crystalline $Pb_9Al_8O_{21}$ has two short bonds at 2.25 and 2.29 Å, and one longer bond at 2.40 Å, and the Pb–O coordination number and the distribution of Pb–O bond lengths in the glasses (see Table 2) suggest a similar three coordinated environment for the lead ions in the glasses. In crystalline $Pb_9Al_8O_{21}$ there are longer Pb–O bonds of length ~2.75 Å, but it is not presently possible to determine whether Pb–O bonds of similar length occur in the glass samples, because of the presence of the much larger O–O peak in the correlation function. The O–O bond length extracted from the neutron correlation function is longer than expected for an AlO_4 tetrahedral unit, and this could be due to longer Pb–O bonds in this region. Such longer Pb–O bonds could arise either from the presence of a proportion of lead ions on symmetric sites, or from longer bonds to the asymmetric sites. In order to determine whether longer Pb–O bonds are present it is necessary to use an experimental technique which yields element-specific information on the correlations and a Pb edge EXAFS experiment is planned.

6. Conclusions

The range of bulk glass formation for the lead aluminate system was found to be from 72.5 to 80.0 mol% PbO. This range is much more restricted than has previously been reported in the literature [1,4]. Neutron diffraction and ^{27}Al MAS NMR studies show that the aluminium in lead aluminate glass is tetrahedrally coordinated, whilst the lead is three coordinated in an asymmetric trigonal pyramid arrangement. The asymmetric distribution of Pb–O distances can be modelled using two bond lengths at ~2.25 Å and ~2.47 Å, with coordination numbers of ~2.4 and ~0.5, respectively. There are similarities to the lead gallate system [9,10] and to the $Pb_9Al_8O_{21}$ crystal structure [25]. The results from both neutron diffraction and Raman scattering indicate that the Pb–O bond lengths become shorter with increasing lead content.

Acknowledgements

This work was funded by EPSRC and the CLRC Center for Materials Physics and Chemistry under Grant CMPC04108, and was partially supported by the United

States National Science Foundation under Grants DMR 0211718 and DMR 0502051.

References

[1] P. Kantor, A. Revcolevschi, R. Collongues, J. Mater. Sci. 8 (1973) 1359.
[2] P. Duwez, R.H. Willens, W. Klement, J. Appl. Phys. 31 (1960) 1136.
[3] R.F. Geller, E.N. Bunting, J. Res. Nat. Bur. Stand. 31 (1943) 257.
[4] H. Morikawa, J. Jegoudez, C. Mazieres, A. Revcolevschi, J. Non-Cryst. Solids 44 (1981) 107.
[5] H. Morikawa, F. Marumo, T. Koyama, M. Yamane, A. Oyobe, J. Non-Cryst. Solids 56 (1983) 355.
[6] P.F. McMillan, W.T. Petuskey, B. Coté, D. Massiot, C. Landron, J.P. Coutures, J. Non-Cryst. Solids 195 (1996) 261.
[7] A.C. Hannon, J.M. Parker, J. Non-Cryst. Solids 274 (2000) 102.
[8] E.-T. Kang, S.-J. Lee, A.C. Hannon, J. Non-Cryst. Solids 352 (2006) 725.
[9] A.C. Hannon, J.M. Parker, B. Vessal, J. Non-Cryst. Solids 196 (1996) 187.
[10] A.C. Hannon, J.M. Parker, B. Vessal, J. Non-Cryst. Solids 232&234 (1998) 51.
[11] Y.G. Choi, K.H. Kim, V.A. Chernov, J. Heo, J. Non-Cryst. Solids 246 (1999) 128.
[12] F. Fayon, C. Bessada, D. Massiot, I. Farnan, J.P. Coutures, J. Non-Cryst. Solids 232–234 (1998) 403.
[13] U. Hoppe, R. Kranold, A. Ghosh, C. Landron, J. Neuefeind, P. Jovari, J. Non-Cryst. Solids 328 (2003) 146.
[14] P. McMillan, B. Piriou, Bull. Miner. 106 (1983) 57.
[15] A.C. Hannon, in: J. Lindon, G. Tranter, J. Holmes (Eds.), Encyclopedia of Spectroscopy and Spectrometry, vol. 2, Academic, London, 2000, p. 1493.
[16] A.C. Hannon, W.S. Howells, A.K. Soper, IOP Conf. Series 107 (1990) 193.
[17] J.E. Kasper, S.A. Feller, G.L. Sumcad, J. Am. Ceram. Soc. 67 (1984) C71.
[18] A.C. Hannon, Nucl. Instrum. Meth. A 551 (2005) 88.
[19] K.J.D. MacKenzie, M.E. Smith, Multinuclear solid-state nuclear magnetic resonance of inorganic materials, in: R.W. Cahn (Ed.), Pergamon Materials Series, Pergamon, Oxford, 2002, p. 740.
[20] A.K. Soper, P. Buchanan, private communication, 2004.
[21] E. Lorch, J. Phys. C 2 (1969) 229.
[22] A.C. Hannon, D.I. Grimley, R.A. Hulme, A.C. Wright, R.N. Sinclair, J. Non-Cryst. Solids 177 (1994) 299.
[23] W.H. Zachariasen, J. Am. Chem. Soc. 54 (1932) 3841.
[24] L. Shimoni-Livny, J.P. Glusker, C.W. Bock, Inorg. Chem. 37 (1998) 1853.
[25] K.B. Plötz, H. Müller-Buschbaum, Z. Anorg. Allg. Chem. 480 (1981) 149.